Design and Performance Evaluation of a Two-Stage Inverter for Grid-Connected PV Systems with Phase Shift Control

M. Nafiah[1], F. Ronilaya[1*], I. N. Syamsiana[1], M. Saputra[1,2]
[1]Faculty of Electrical Engineering, State Polytechnic of Malang, Jalan Soekarno-Hatta No. 9, Malang, Indonesia
[2] PEMC Research Institute, The University of Nottingham, NG7 2RD, United Kingdom
[*]corresponding author's email: ferdian@polinema.ac.id

Abstract – *This study investigates the design and performance evaluation of a two-stage inverter for grid-connected photovoltaic (PV) systems using the phase shift control meth-od (power angle). In this method, the inverter output voltage waveform is controlled to lead the grid voltage. The series inductance between the inverter and the grid is optimally designed to ensure that the injected current has a low total harmonic distortion (THD). The hardware is implemented using an Arduino microcontroller with a look-up table-based Sinusoidal Pulse Width Modulation (SPWM) method, complemented by a zero-cross detector to ensure grid synchronization. Phase angle variations from 0° to 80° were tested to analyze their impact on the injected power. The test results indicate that increasing the phase angle leads to higher active power being injected into the grid, although it has no significant impact on reactive power injection. Additionally, the results show that a larger power angle also improves the system's power factor. Therefore, this approach can be used as an alternative strategy for managing power injection from solar PV systems within the concept of dispatchable PV inverters.*

Keywords: *grid synchronization, phase shift control, power, total harmonic distortion, two-stage inverter*

Article History
Received 02 August 2025
Received in revised form 25 May 2026
Accepted 22 June 2026
Published Online October 2026

I. Introduction

Electricity is a fundamental necessity in modern society. In Indonesia, fossil fuels still play a dominant role in electricity generation. As of 2018, the majority of the country's power generation capacity was derived from fossil energy sources, with coal accounting for approximately 50%, followed by natural gas (29%), oil (7%), and renewable energy (14%) [1]. This reliance underscores the urgent need for coordinated efforts among public, private, and governmental sectors to reduce dependence on finite fossil fuel resources. Positioned along the equatorial line, Indonesia possesses significant solar energy potential, receiving an average daily solar irradiation of approximately 4.8 kWh/m² with a tolerance of ±9%. Harnessing this potential is crucial for decreasing future reliance on fossil-based energy. However, considering the high capital investment required for solar power systems, optimizing their performance through effective power control strategies is essential to ensure long-term feasibility and efficiency.

The adoption of renewable energy sources for electricity generation has steadily increased due to their diversity and ability to support utility grids. Among these technologies, grid-connected inverters serve a critical function in managing energy flow and ensuring seamless integration with the electrical grid. In photovoltaic (PV) systems, inverters are essential components that enable optimal power delivery to the grid while ensuring compliance with established grid standards [2]–[4]. In addition to the inverter stage, DC-DC converters are required to regulate the variable DC output generated by solar modules. These converters play a vital role in stabilizing the PV voltage and improving overall system performance, thereby making them a key element in the design of efficient inverter architectures.

The topologies of commercial and industrial photovoltaic (PV) inverters have continuously evolved to enhance efficiency, reduce cost, and minimize size and weight compared to isolated inverter designs. Additionally, effective PV array configurations contribute to improved performance, particularly under partial shading conditions. Among available architectures, single-stage microinverters are often preferred for their simplicity and compact form factor. However, dual-stage inverter designs offer more flexible and robust control strategies, which can lead to improved dynamic performance and grid compliance [5].

This is an Open Access article distributed under the terms of the Creative Commons Attribution 4.0 International License, permitting copy and redistribution of the material and adaptation for commercial and uncommercial use.

Previous research by Ronilaya et al. in 2019 proposed an alternative method to maximize PV power using a simple technique combining a Sepic converter and a fly-back-type inverter for optimal power flow control in small-scale grid-connected PV systems. Their results indicated that a microinverter controlled with an incremental conductance (IC) MPPT method exhibited satisfactory performance and higher efficiency compared to non-MPPT methods [6].

In 2019, Ronilaya et al. introduced a grid-connected inverter with VAr support capabilities for small-scale solar PV systems. Reactive power control was implemented using a droop technique and a phase-locked loop for synchronization between the inverter and the grid. A full-bridge voltage source inverter was employed in this research [7].

In 2021, Ronilaya et al. discussed inverter control strategies for small-scale grid-connected PV systems. The control scheme employed power angle adjustment and voltage regulation approaches, with power angles adjustable between 0 and 90 degrees. Results indicated that active and reactive power injected into the grid significantly depended on power angle variations, with a larger power angle leading to a power factor closer to 1. Voltage control had minimal impact on active power flow but influenced reactive power flow [8].

Another study proposed a topology using an LLC resonant converter with a high-frequency isolation transformer in the DC-DC stage. The output of this stage produced sinusoidal voltage and current waves, which were rectified at grid frequency. Phase-shift and frequency control methods were employed to synchronize with the reference current signal over the operational range [9].

Ronilaya et al. also explored a two-stage inverter topology using four MOSFET switches to convert DC voltage into AC. The system utilized an Arduino UNO micro-controller for SPWM signal generation, producing a pure sinusoidal wave output of 220V at 50 Hz. This design achieved high efficiency in terms of circuit operation [4], [10], [11], [12].

Based on the problems and literature review, previous research has not specifically addressed phase aspect in two-stage topologies connected to on-grid systems. While prior studies focused on phase shift control, they did not explore two-stage topology or voltage control in on-grid inverters. This research aims to design an inverter with maximum efficiency through optimized control, emphasizing circuit topology and synchronization methods in on-grid systems. It is expected to enhance the adoption and understanding of renewable energy in Indonesia and significantly contribute to developing grid-connected PV technologies, particularly in flexible PV power regulation.

II. The Control Strategy

An inverter connected to the grid can be represented by an equivalent circuit, as shown in Fig. 1. The reactor, with an equivalent resistance R_3 and inductance L_3, connects the inverter to the grid with an impedance expressed as $Z_3=R_3+jX_3$, where θ is the phase angle of the impedance Z_3. The inverter output voltage is denoted as $V_i\angle 0°$, while the grid voltage is represented as $V_g\angle -\delta$, and the current injected by the inverter into the grid is expressed as $I\angle\phi$. The power delivered from the inverter to the grid is defined by (1). Equations (2) and (3) represent the active and reactive power, respectively, that result from separating the real and imaginary components of (1) [13], [14], [15].

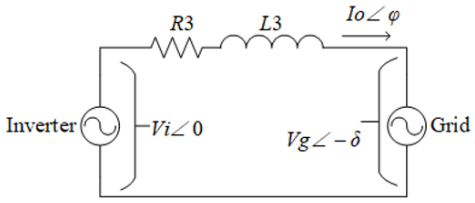


Fig. 1. The equivalent circuit of grid-connected inverter

$$\overline{S} = \overline{V}_i \times \overline{I}^* = (V_i\angle 0)\left(\frac{V_i\angle 0 - V_g\angle -\delta}{Z_3\angle\theta}\right)^* \quad (1)$$

$$P = \frac{V_i^2}{Z_3}\cos\theta - \frac{V_iV_g}{Z_3}\cos(\delta+\theta) \quad (2)$$

$$Q = \frac{V_i^2}{Z_3}\sin\theta - \frac{V_iV_g}{Z_3}\sin(\delta+\theta) \quad (3)$$

In medium and high-voltage power systems, the reactance is significantly greater than the resistance ($X \gg R$). Therefore, the resistance value is neglected. By assuming a small value for δ, where $\sin\delta$ is approximately equal to δ, (2) and (3) can be transformed into:

$$P = \frac{V_iV_g}{X_3} sin\ \delta = P = \frac{V_iV_g}{X_3}\ \delta \quad (4)$$

$$Q = \frac{V_i(V_i - V_g cos\ \delta)}{X} = \frac{V_i(V_i - V_g)}{X} \quad (5)$$

In medium and high voltage systems, δ significantly influences the active power output, whereas the inverter voltage influences the reactive power output, as demonstrated by (4) and (5). On the other hand, low voltage systems operate differently. The reactance can be ignored in low voltage systems since the resistance is greater than the reactance ($R \gg X$). The results are $\sin\delta = \delta$ and $\cos\delta = 1$ if it is assumed that δ is very small. Equations (6) and (7) provide the power flow equations [15]. From (4) to (7), it can be observed that Vi and δ are two parameters that can be used for power regulation.

$$P = \frac{V_i}{R}\left(V_i - V_g\right) \quad (6)$$

$$Q = -\frac{V_iV_g}{R}\delta \quad (7)$$

III. The System Topology

A. The circuit topology of two-stage inverter

In a two-stage inverter, the DC-DC converter serves as the link between the PV panel and the DC/AC inverter. The PV panel converts sunlight into DC electricity, and for PV panels with low output voltage, a DC-DC boost converter is employed. DC/DC power converters are used in PV systems to modify the output voltage. Typically, DC/DC converters are placed in series between the load and the PV panel to extract the available power from the panel through a tracking method. This approach is beneficial for PV systems with unstable and fluctuating output. The DC voltage is then converted into AC voltage using a power electronics system (inverter). In PV applications, a well-designed inverter controller is crucial for enhancing inverter performance since the conversion process relies on control algorithms [16], [17], [18]. A typical two-stage boost inverter consists of a DC-DC boost converter, an H-bridge inverter, and an output filter.

As illustrated in Fig. 2, the concept of a two-stage topology inverter consists of two main stages. The first stage is DC-DC conversion, and the second stage is DC-AC conversion. In the first stage, low DC voltage from sources such as solar panels, batteries, or other power sources is boosted to a higher DC voltage using a DC-DC boost converter. This boost converter operates based on the principles of inductance and capacitance, where energy is temporarily stored in the inductor and then released at a higher voltage through rapid switching regulation [4], [19]. The use of Pulse Width Modulation (PWM) control in the boost converter enables precise regulation of the desired output voltage and enhances conversion efficiency.

In the second stage, the boosted DC voltage is converted into AC voltage using an inverter. This inverter often employs switching techniques, such as PWM, to produce a smooth and stable sinusoidal wave, meeting the requirements of end-use applications such as household appliances or industrial systems. By separating the voltage boosting and AC conversion processes into two distinct stages, this topology allows better control of each process while improving overall efficiency and the quality of the generated power [20], [21].

This type of inverter is typically used as an interface between renewable energy sources, batteries, fuel cells, and the grid. It can also be applied to motors powered by batteries or fuel cells. Since the voltage of these power sources is often uncertain and variable, the role of the DC-DC converter is to regulate the DC-link voltage V_{dc} to a desired constant value for easier control and improved inverter performance. Additionally, the DC-DC boost converter serves the purpose of enabling lower source voltage for safety reasons [22].

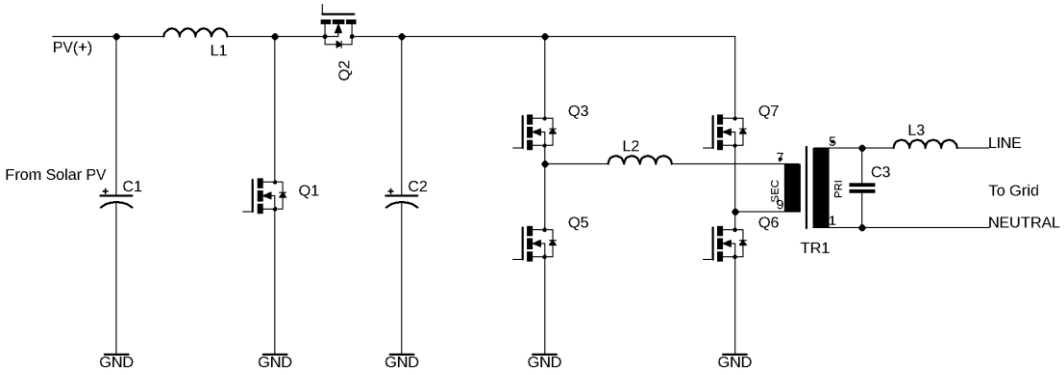


Fig. 2. Topology of two-stage inverter

B. The block diagram of the proposed system

Fig. 3 shows the block diagram of the proposed system. The system begins with solar PV panels generating DC power, which is then stepped up by the boost converter. The two-stage inverter topology converts DC into synchronized AC power. Control signals generated by the Arduino Nano, utilizing SPWM through a lookup table, are transmitted to the driver circuit (IR2110 ICs), which drives the inverter switches. To ensure grid synchronization, a zero-cross detector (IC LM358) and phase control circuit (IC LM741) work together to monitor and adjust the phase relationship between the inverter and the grid. The step-up transformer and LC filter optimize the voltage level and wave quality, respectively [23]. Finally, the conditioned power is injected into the grid with minimal distortion.

C. The phase-shifter, zero cross detector & driver circuit

The Phase Control circuit is designed to generate a sinusoidal waveform leading by 0° to 80° degrees with respect to the sinusoidal voltage waveform of the utility grid. This circuit consists of an LM741 IC, resistors, a potentiometer, and a capacitor, as shown in Fig. 4. The output at pin 6 of the LM741 IC, labeled as OP-AMP1-OUT, is connected to the input at pin 2 of the zero-cross detector circuit. The input for the phase shift

circuit is obtained from the terminals of the step-down transformer [24].

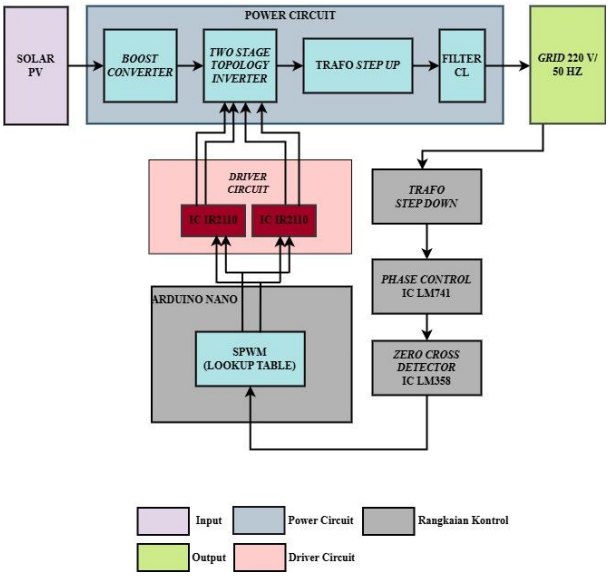


Fig. 3. The block diagram of the proposed system

The Zero Crossing Detector circuit functions to track or detect when the grid voltage waveform crosses the zero (zero-crossing) during its sinusoidal cycle. The primary purpose of this circuit is to identify the zero-crossing points on the sinusoidal waveform. This circuit consists of an LM358 IC, resistors, diodes, and a potentiometer, as shown in Fig. 5. The input at pin 2 of the LM358 IC receives input from OP-AMP1-OUT of the previous phase shift circuit. The zero-crossing detector is often used in power control systems to synchronize or regulate the generation of PWM (Pulse Width Modulation) signals to control electronic devices in power systems. By detecting the zero-crossing points of the waveform, the output voltage frequency of the inverter will always match the grid voltage frequency [25], [26], [27], [28].

The driver circuit shown in Fig. 6 functions as an amplifier to boost the output voltage of the SPWM circuit from 5V to ±10V, as MOSFETs operate at a gate voltage of approximately ±10V. In this study, the design and implementation of the driver circuit utilize the IR2110.

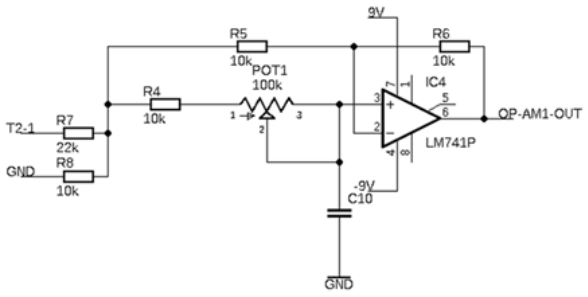


Fig. 4. The phase-shifter circuit

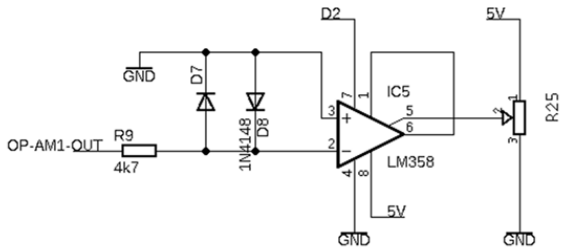


Fig. 5. The zero cross detector circuit

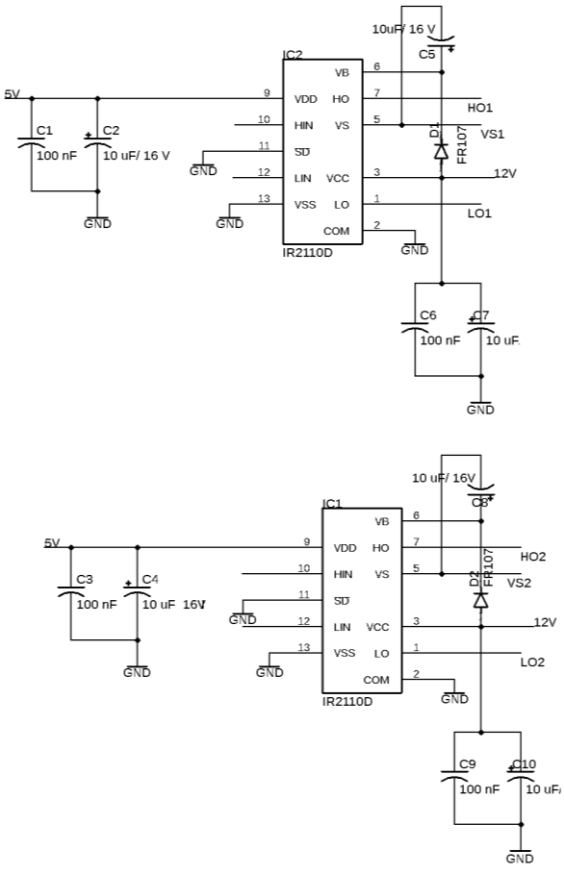
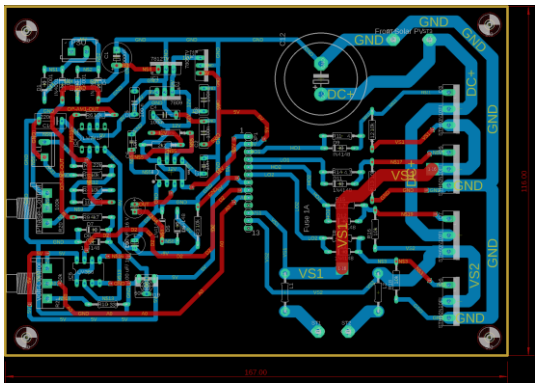


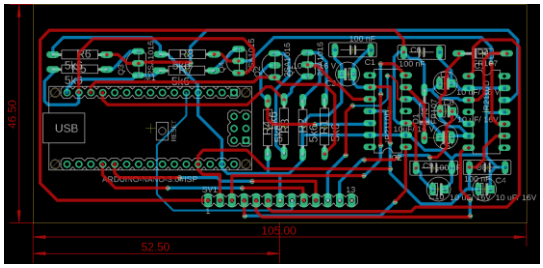
Fig. 6. The MOSFET driver circuit

D. The circuit implementation

Fig. 7(a) and (b) shows PCB layout for the inverter circuit and controller circuit respectively. The layout emphasizes minimizing power loss and ensuring efficient energy transfer, as given by optimized trace routing for high-current paths and the placement of high-frequency capacitors close to the switching devices MOSFET Q_1 to Q_4. Fig. 8 shows the overall hardware installation of the inverter system.



(a)



(b)

Fig. 7. (a) PCB layout for the converter, (b) PCB layout for the controller

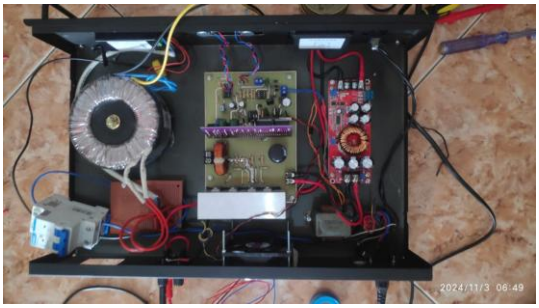
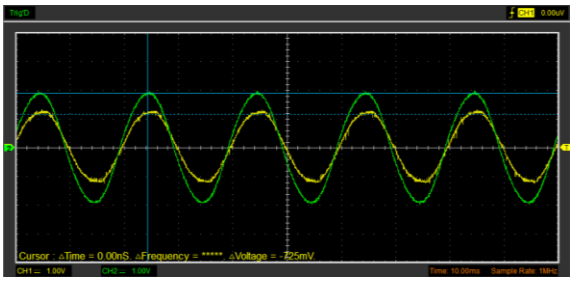


Fig. 8. Hardware implementation

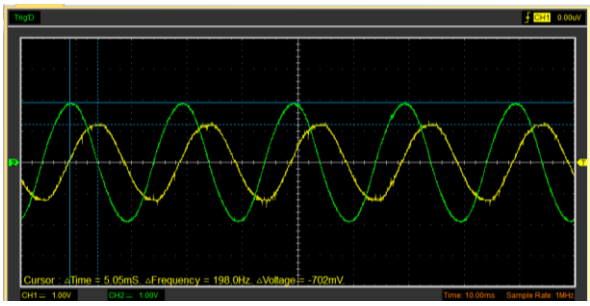
IV. Experiment and result discussion

A. Testing and Validation of Inverter Subsystem Components

The testing of the inverter is conducted to ensure its performance meets the required standards. The process begins with sectional testing, starting from the phase shifter circuit, the microcontroller outputs for each MOSFET and bridge inverter output. Fig. 9 shows the test results of the phase shifter circuit. Fig. 9(a) depicts the voltage waveforms of the inverter and the grid when the phase difference is 0°, while Fig. 9(b) shows the waveforms when the phase difference is 90°.



(a)



(b)

Fig. 9. (a) Voltage waveforms of an inverter and grid when the power angle is 0° (b) Voltage waveforms of an inverter and grid when the power angle is 90°

The test results of the SPWM lookup table designed for MOSFETs Q_1 and Q_3 are shown in Fig. 10, while the gate driver signals for MOSFETs Q_2 and Q_4 are shown in Fig. 11. The switching frequency for the waveform in Fig. 10 is 10 kHz, whereas the PWM signal in Fig. 11 has a frequency of 50 Hz. MOSFETs Q_1 and Q_3 are positioned on the high side, while Q_2 and Q_4 are on the low side of the inverter circuit. The output waveform of the bridge inverter before filter is given by Fig. 12.

Several key parameters are carefully considered during the testing. The grid voltage is 220 V with a frequency of 50 Hz, and the inverter output voltage is adjusted to be 5 V higher than the grid voltage. This adjustment prevents reverse power flow from the grid to the solar PV during the initial connection and is achieved by fine-tuning the potentiometer to achieve the desired voltage level.

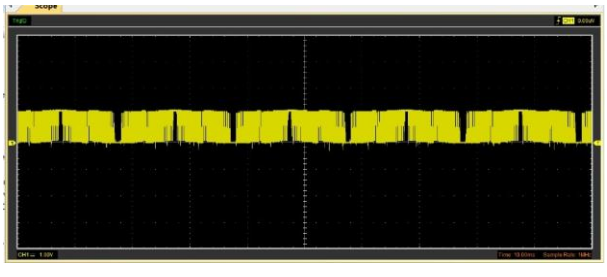


Fig. 10. The gate driver signal for MOSFETs Q1 and Q3.

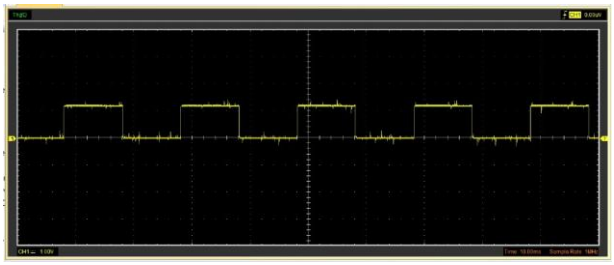


Fig. 11. The gate driver signal for MOSFETs Q2 and Q4.

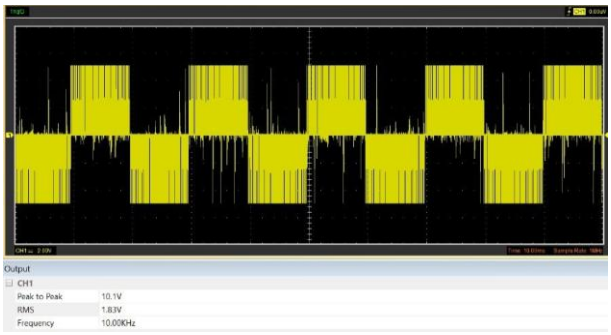


Fig. 12. The output waveform of the bridge inverter before filter

The maximum power deliverable by the inverter is limited to 150 W, corresponding to the output of a single solar panel. When connecting the inverter to the grid, it is crucial to ensure that the phase angle difference between the inverter voltage and the grid voltage is 0 degrees. A step-up transformer with a 10 A capacity is utilized to facilitate the voltage transformation. Additionally, the Total Harmonic Distortion (THD) of the inverter voltage must be maintained below 5% to ensure compliance with power quality standards. Fig. 13 shows the inverter voltage waveform after being filtered using a 10 mH series inductor and a 2.2 µF capacitor, while Fig. 14 depicts the voltage harmonic profile, indicating a THD value of 1.6%, which complies with the maximum standard of 5%.

B. Grid-connected test

To analyze the impact of power angle variation on the inverter's performance, the potentiometer (see Fig. 4) controlling the phase shifter is adjusted, and key parameters such as voltage, current, active power, power factor, and THD are recorded. This structured approach ensures that the inverter operates safely and aligns with the technical requirements for grid connection.

Fig. 15 illustrates the relationship between power angle and power factor for two different inverter voltage settings: 237 V and 250 V. Generally, the power factor increases as the power angle rises from 10° to approximately 50° for both voltage settings, indicating a positive correlation in this range. Beyond 50°, the power factor stabilizes, showing minimal variation with further increases in the power angle.

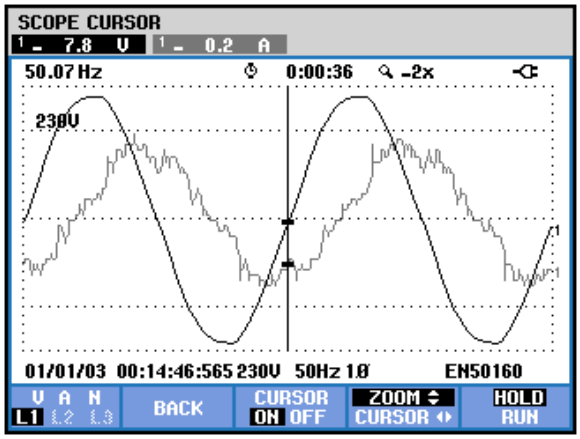


Fig. 13. The output waveform of the inverter after filter

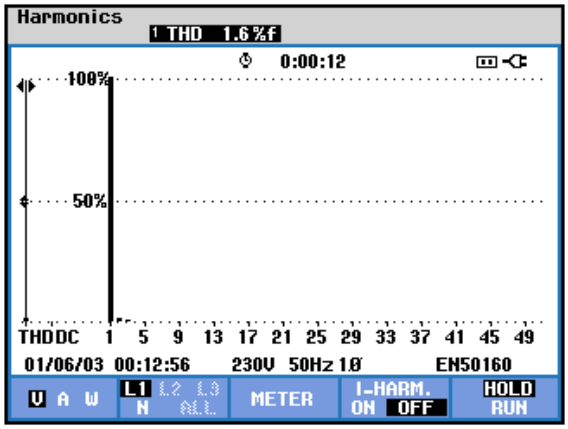


Fig. 14. The voltage harmonic profile

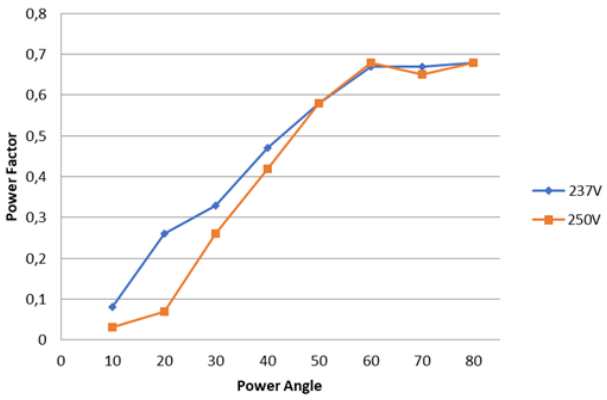


Fig. 15. The power factor profile under varied power angle

At lower power angles (10° to 30°), the power factor for the 250 V setting is lower compared to 237 V, suggesting that the higher voltage setting results in a slower initial improvement in power factor. However, from 40° to 50°, the power factors for both voltage settings converge, demonstrating similar performance. Beyond 50°, the power factors for both settings become nearly identical, stabilizing around 0.6 to 0.7.

The voltage setting of 237 V achieves a higher power factor earlier in the power angle range (10° to 30°), indicating potentially better efficiency at smaller power angles. On the other hand, the delayed rise in power factor for the 250 V setting at lower angles may result from higher losses or delayed phase alignment between voltage and current. Nevertheless, at higher power angles, the influence of the voltage setting diminishes, leading to similar power factor performance for both settings.

From a practical standpoint, operating at a power angle of approximately 50° to 60° optimizes the power factor for both voltage settings, making this range ideal for efficient operation regardless of the inverter voltage. For applications requiring efficient operation at lower power angles, the 237 V setting might be more advantageous. This analysis highlights the importance of selecting appropriate power angles and voltage levels to achieve optimal power factor performance.

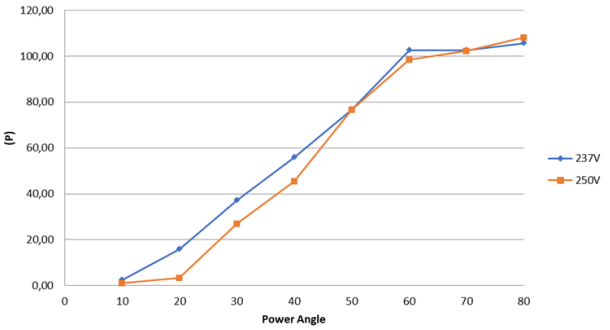


Fig. 16. The active power profile under varied power angle

Fig. 16 depicts the relationship between power angle and active power *P* for two inverter voltage settings: 237 V and 250 V. As the power angle increases, active power rises for both voltage settings, demonstrating a strong positive correlation between these variables. The active power increases more rapidly at smaller power angles (10° to 40°), while the rate of increase slows and stabilizes as the power angle approaches 80°. For smaller power angles, the sine function (sin δ) behaves almost linearly since for small values of δ (in radians), sin δ ≈ δ. This linear approximation implies that the active power *P* increases proportionally with the power angle, complies with above (4).

This explains why the graph shows a rapid increase in active power at smaller angles. The relationship between *P* and δ appears nearly linear, resulting in a steeper slope in the graph within this range. As the power angle increases beyond 40°, the sine function (sin δ) starts to exhibit non-linear behavior. The rate of increase in active power begins to slow down because sin δ approaches its maximum value of 1 as δ nears 90°. The derivative of the power equation is:

$$\frac{dP}{d\delta} = \frac{V_i V_g}{X_3} \cos\delta \tag{8}$$

It shows that the rate of change of power d*P*/dδ depends on cos δ. As δ increases, cos δ decreases, causing d*P*/dδ to approach zero. This results in a slower rate of power increase, as observed in the graph.

For most of the power angle range, the active power for the 237 V setting is slightly higher than that of the 250 V setting. This difference is more pronounced at lower power angles, where the 237 V setting delivers more active power. From 50° onwards, the active power values for both voltage settings converge, eventually becoming nearly identical at higher power angles. The higher active power output at 237 V in the lower power angle range could indicate that this voltage setting is more efficient in transferring active power at smaller angles. However, as the power angle increases, the performance of both voltage settings aligns, suggesting that the influence of voltage diminishes at higher angles.

V. Conclusions

This study investigated the design and performance evaluation of a two-stage inverter for grid-connected photovoltaic (PV) systems using the phase shift control method (power angle). This study demonstrates that the phase shift control method effectively regulates active power injection and influences the power factor in grid-connected two-stage PV systems. Experimental evaluation reveals that the power angle exhibits a strong positive correlation with both performance metrics. Specifically, the power factor improves steadily between 10° and 50° across different grid voltage levels (237 V and 250 V) before stabilizing around 0.6 to 0.7. Meanwhile, active power injection increases rapidly and nearly linearly within the 10° to 40° range, governed by the sine function behavior. Beyond 40°, this increase decelerates, reaching stagnation as the angle approaches 80°.

These hardware-based findings confirm that the 10° to 40° range is optimal for predictable and linear power dispatch. Conversely, operating beyond 80° leads to power reduction and system inefficiency. To ensure long-term stability and reliability in practical applications, future research must prioritize the development of specialized protection mechanisms for grid-connected PV systems when operating angle accidentally exceeds the 80° threshold.

Acknowledgements

This work was supported by a research grant from the Ministry of Education, Culture, Research, and Technology of the Republic of Indonesia, based on Decree No. 17/D4/O/2024 and Contract Agreement No. 72/ SPK/D.D4/PPK.01.APTV/III/2024.

Conflict of Interest

The authors declare no conflict of interest in the publication process of the research article.

Author Contributions

Author 1 conducted the experiments, collected and analyzed the data, and drafted the original manuscript. Author 2 conceptualized the research framework, supervised the study, provided resources, and critically revised the manuscript. Author 3 contributed to the methodology, validated the experimental results, and co-supervised the project. Author 4 performed formal language editing, proofreading, and technical writing review.

References

[1] Sekretariat Jenderal Dewan Energi Nasional, "Outlook Energi Indonesia (OEI) 2019," 2019.

[2] E. Mohammadi, M. Rezvanyvardom, and A. Mirzaei, "Soft switching high step-up three-level boost DC-DC converter with Quasi Z-source for Photovoltaic application," Computers and Electrical Engineering, vol. 116, p. 109159, 2024, doi: https://doi.org/10.1016/j.compeleceng.2024.109159.

[3] Y. Chen, M. Xu, W. Xiao, B. Zhang, and D. Qiu, "General method for constructing multi-input high-boost DC-DC converters with low spike current," International Journal of Circuit Theory and Applications, vol. 50, no. 8, pp. 2847–2864, Aug. 2022, doi: https://doi.org/10.1002/cta.3294.

[4] A. Mondzik, R. Stala, S. Pirog, A. Penczek, P. Gucwa, and M. Szarek, "High Efficiency DC-DC Boost Converter with Passive Snubber and Reduced Switching Losses," IEEE Transactions on Industrial Electronics, vol. 69, no. 3, pp. 2500–2510, Mar. 2022, doi: 10.1109/TIE.2021.3063874.

[5] E. Heydari, A. Y. Varjani, and D. Diallo, "A Dual-Function Power Decoupling Circuit for Single-Stage Grid-Connected PV Inverter," IEEE Trans Power Electron, vol. 37, no. 6, pp. 7422–7431, 2022, doi: 10.1109/TPEL.2022.3143951.

[6] F. Ronilaya et al., "A double stage micro-inverter for optimal power flow control in grid connected PV system," in 2018 International Conference on Information and Communications Technology (ICOIACT), 2018, pp. 808–813. doi: 10.1109/ICOIACT.2018.8350788.

[7] F. Ronilaya, W. Anistia, I. N. Syamsiana, I. Siradjuddin, M. Junus, and Aripriharta, "A Grid-connected Inverter with VAr Support Capability for A Small Scale Solar PV Using A Droop Technique," in 2019 International Conference on Technologies and Policies in Electric Power & Energy, 2019, pp. 1–6. doi: 10.1109/IEEECONF48524.2019.9102585.

[8] F. Ronilaya, M. Hapidi, S. Wibowo, R. I. Putri, A. Zuhroh, and A. R. Putro, "A Flexible Power Flow Control of a Voltage Source Inverter for a Grid-Connected 100 Wp Solar PV Application," in 2021 IEEE 5th International Conference on Information Technology, Information Systems and Electrical Engineering (ICITISEE), 2021, pp. 163–168. doi: 10.1109/ICITISEE53823.2021.9655931.

[9] N. Altin, S. Ozdemir, M. Khayamy, and A. Nasiri, "A Novel Topology for Solar PV Inverter Based on an LLC Resonant Converter With Optimal Frequency and Phase-Shift Control," IEEE Trans Ind Appl, vol. 58, no. 4, pp. 5042–5054, 2022, doi: 10.1109/TIA.2022.3163372.

[10] Y. Wang and R. Li, "Novel High-Efficiency Three-Level Stacked-Neutral-Point-Clamped Grid-Tied Inverter," IEEE Transactions on Industrial Electronics, vol. 60, no. 9, pp. 3766–3774, 2013, doi: 10.1109/TIE.2012.2204712.

[11] W. Yu, J.-S. J. Lai, H. Qian, and C. Hutchens, "High-Efficiency MOSFET Inverter with H6-Type Configuration for Photovoltaic Nonisolated AC-Module Applications," IEEE Trans Power Electron, vol. 26, no. 4, pp. 1253–1260, Apr. 2011, doi: 10.1109/TPEL.2010.2071402.

[12] Z. Liang, R. Guo, J. Li, and A. Q. Huang, "A High-Efficiency PV Module-Integrated DC/DC Converter for PV Energy Harvest in FREEDM Systems," IEEE Trans Power Electron, vol. 26, no. 3, pp. 897–909, Mar. 2011, doi: 10.1109/TPEL.2011.2107581.

[13] N. Mohammed, A. Lashab, M. Ciobotaru, and J. M. Guerrero, "Accurate Reactive Power Sharing Strategy for Droop-Based Islanded AC Microgrids," IEEE Transactions on Industrial Electronics, vol. 70, no. 3, pp. 2696–2707, 2023, doi: 10.1109/TIE.2022.3167141.

[14] W. Cao, M. Han, X. Zhang, Y. Guan, J. M. Guerrero, and J. C. Vasquez, "An Integrated Synchronization and Control Strategy for Parallel-Operated Inverters Based on V–I Droop Characteristics," IEEE Trans Power Electron, vol. 37, no. 5, pp. 5373–5384, 2022, doi: 10.1109/TPEL.2021.3135461.

[15] B. Fan et al., "A Novel Droop Control Strategy of Reactive Power Sharing Based on Adaptive Virtual Impedance in Microgrids," IEEE Transactions on Industrial Electronics, vol. 69, no. 11, pp. 11335–11347, 2022, doi: 10.1109/TIE.2021.3123660.

[16] A. R. Gautam, D. M. Fulwani, R. R. Makineni, A. K. Rathore, and D. Singh, "Control Strategies and Power Decoupling Topologies to Mitigate 2ω-Ripple in Single-Phase Inverters: A Review and Open Challenges," IEEE Access, vol. 8, pp. 147533–147559, 2020, doi: 10.1109/ACCESS.2020.3015315.

[17] B. A. Ador and M. T. Zaman, "A Review of the DC-AC Inverters Used in Photovoltaic Systems," in 2023 IEEE 9th International Women in Engineering (WIE) Conference on Electrical and Computer Engineering (WIECON-ECE), 2023, pp. 13–18. doi: 10.1109/WIECON-ECE60392.2023.10456415.

[18] Y. P. Siwakoti and F. Blaabjerg, "Common-Ground-Type Transformerless Inverters for Single-Phase Solar Photovoltaic Systems," IEEE Transactions on Industrial Electronics, vol. 65, no. 3, pp. 2100–2111, 2018, doi: 10.1109/TIE.2017.2740821.

[19] D.-Y. Jung, Y.-H. Ji, S.-H. Park, Y.-C. Jung, and C.-Y. Won, "Interleaved Soft-Switching Boost Converter for Photovoltaic Power-Generation System," IEEE Trans Power Electron, vol. 26, no. 4, pp. 1137–1145, Apr. 2011, doi: 10.1109/TPEL.2010.2090948.

[20] M. Shayestegan, "Overview of grid-connected two-stage transformer-less inverter design," Journal of Modern Power Systems and Clean Energy, vol. 6, no. 4, pp. 642–655, 2018, doi: 10.1007/s40565-017-0367-z.

[21] G. M. Jagadeesan, R. Pitchaimuthu, and M. Sridharan, "A Two-stage Single-phase Grid-connected Solar-PV System with Simplified Power Regulation," Chinese Journal of Electrical Engineering, vol. 8, no. 1, pp. 81–92, Mar. 2022, doi: 10.23919/CJEE.2022.000008.

[22] S.-M. Chen, T.-J. Liang, L.-S. Yang, and J.-F. Chen, "A Safety Enhanced, High Step-Up DC–DC Converter for AC Photovoltaic Module Application," IEEE Trans Power Electron, vol. 27, no. 4, pp. 1809–1817, Apr. 2012, doi: 10.1109/TPEL.2011.2170097.

[23] Z. Lin, J. Jiang, S. Pan, J. Gong, F. Liu, and L. Yao, "A Single-Phase Nonisolated Inverter With a High Attenuation Gain Magnetic-Coupled Active Filter," IEEE Trans Power Electron, vol. 38, no. 12, pp. 15719–15730, 2023, doi: 10.1109/TPEL.2023.3311399.

[24] Quan Li and P. Wolfs, "A Review of the Single Phase Photovoltaic Module Integrated Converter Topologies With Three Different DC Link Configurations," IEEE Trans Power Electron, vol. 23, no. 3, pp. 1320–1333, May 2008, doi: 10.1109/TPEL.2008.920883.

[25] Y. Tang, C. Zhang, Y. Guo, H. Sun, and L. Jiang, "Optimization of Zero-Crossing Distortion for Unipolar BCM Grid-Tied Inverter," IEEE J Emerg Sel Top Power Electron, vol. 11, no. 4, pp. 3680–3691, 2023, doi: 10.1109/JESTPE.2022.3179783.

[26] A. Kotsopoulos, P. J. M. Heskes, and M. J. Jansen, "Zero-crossing distortion in grid-connected PV inverters," IEEE Transactions on Industrial Electronics, vol. 52, no. 2, pp. 558–565, 2005, doi: 10.1109/TIE.2005.844254.

[27] A. Kotsopoulos, P. J. M. Heskes, and M. J. Jansen, "Zero-crossing distortion in grid-connected PV inverters," in IEEE 2002 28th Annual Conference of the Industrial Electronics Society. IECON 02, 2002, pp. 1101–1106 vol.2. doi: 10.1109/IECON.2002.1185426.

[28] M. Chen, Z. Ye, Y. Chen, and D. Xu, "Zero-Voltage-Switching Single-Phase Full-Bridge Inverter With Active Power Decoupling," IEEE Trans Power Electron, vol. 36, no. 1, pp. 571–582, 2021, doi: 10.1109/TPEL.2020.2998640.